Self-Organized Lateral Ordering in Vertically Aligned PbSe Quantum Dot Superlattices

G. Springholz, A. Raab, R.T. Lechner
Institut für Halbleiter- und Festkörperphysik,
Johannes Kepler Universität, A-4040 Linz, Austria

Self-organized lateral ordering is studied for vertically aligned self-assembled PbSe/ $Pb_{1-x}Eu_xTe$ quantum dot superlattices. It is found that a pronounced hexagonal lateral ordering tendency exists for $Pb_{1-x}Eu_xTe$ spacer thicknesses around 160 Å with a resulting narrowing of the size distribution. In addition, the in-plane dot separations and the dot density are tunable by changes in the spacer thickness with an almost two-fold density increase for spacer thicknesses from 100 to 275 Å. Similar marked changes are also found for PbSe dot shapes as well as the dot sizes. This provides additional means for the tuning of the optical and electronic properties of the dots.

1. Introduction

Self-organization during strained-layer heteroepitaxy of self-assembled quantum dot superlattices has recently been shown to result in the formation of vertically and laterally ordered dot superstructures [1] – [3]. This is based on the elastic interaction between the dots on the surface and the buried dots during superlattice growth [1], [2]. Experimentally, different types of dot arrangements have been observed for different materials systems [1], [2]. This is due to the strong influence of the elastic anisotropy and the growth orientation on these interactions [3]. The PbSe/$Pb_{1-x}Eu_xTe$ system is unique in this respect because different vertical and lateral correlations can be obtained in the superlattices just by changes in the spacer thickness [4]. In particular, either an *fcc*-like stacking or a vertical dot alignment is obtained for spacer thicknesses either larger or smaller than about 380 Å. For the *fcc*-stacked superlattices, a highly efficient lateral ordering mechanism was found in our previous work [2] which results in significant dot size homogenization [5]. Based on such structures we have recently fabricated mid-infrared vertical cavity surface emitting PbSe quantum dot lasers [6]. In the present work, it is demonstrated that also for the vertically aligned PbSe dot superlattices a pronounced hexagonal lateral ordering tendency exists. This ordering process strongly depends on the $Pb_{1-x}Eu_xTe$ spacer thickness, and is most pronounced for spacer thicknesses around 150 Å, leading to a narrowing of the size distribution. Marked changes are also found for the PbSe dot shapes as well as the dots size. This provides additional means for the tuning of the optical and electronic properties of the dots for device applications.

2. Experimental

The samples were grown by molecular beam epitaxy onto 1.5 μm PbTe buffer layers predeposited on (111) BaF_2 substrates. Each superlattice (SL) consists of 50 periods of 5 monolayers (ML) PbSe alternating with $Pb_{1-x}Eu_xTe$ spacer layers with varying thickness but constant Eu concentration of 8%. Due to the corresponding -5.4% PbSe/ $Pb_{1-x}Eu_xTe$ lattice-mismatch, strain-induced coherent 3D islands are formed in each PbSe layer

when the thickness exceeds 1.5 monolayers (ML). For all samples a substrate temperature of 360°C and growth rates of 0.12 and 1 ML/sec for PbSe and $Pb_{1-x}Eu_xTe$ were used, respectively. For the investigation of the lateral ordering process a series of superlattice samples was prepared with $Pb_{1-x}Eu_xTe$ spacer layers varying from 80 to 330 Å. This is the range of spacer thicknesses where the PbSe dots are aligned vertically along the growth direction. After growth, all samples were analyzed by high resolution x-ray diffraction and by contact-mode atomic force microscopy. Statistical information on the dot size distributions and the lateral ordering tendency was obtained by means of a special image processing software.

3. Results

For superlattices with spacer thicknesses of 105 to 330 Å, representative AFM images are shown in Fig. 1 a) to e). As compared to the completely disordered dot arrangement of the single dot reference layer (see Fig. 1 f)), in the superlattices there is a clear tendency for a lateral alignment of the dots along the in-plane <-110> surface directions. As a result, a 2D hexagonally ordered dot arrangement is formed, which is directly evidenced by the appearance of six-fold symmetric satellite peaks in the Fourier transform (FFT) power spectra of the AFM images shown as inserts in Fig. 1. In addition, the dot sizes and spacings in the superlattices are much larger as those of the single dot reference layer, and the spacing and size continuously increase with increasing spacer thickness. In the FFT power spectra of Fig. 1, this is reflected by the corresponding decrease in the FFT satellite peak separations.

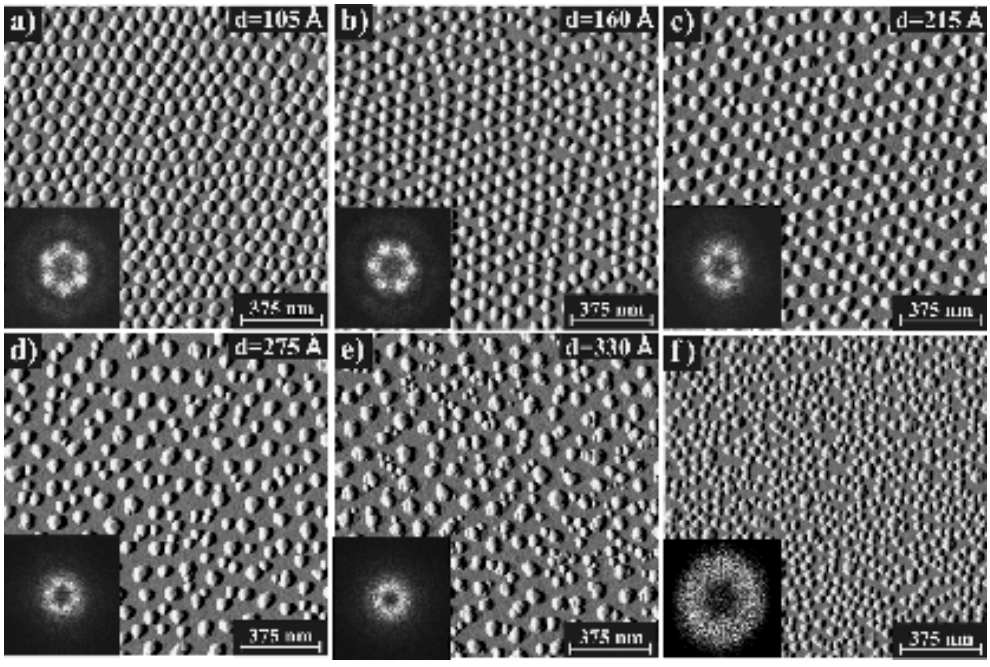

Fig. 1: AFM surface images of PbSe/$Pb_{1-x}Eu_xTe$ quantum dot superlattices (50 periods) with varying $Pb_{1-x}Eu_xTe$ spacer thicknesses of 105, 160, 215, 275 and 330 Å, from a) to e), respectively. (f) AFM image of a 5 ML single PbSe dot reference layer. Inserts: 2D FFT power spectra of the AFM images.

Even more striking is the fact that the best lateral dot order is formed for the superlattices with spacer thicknesses in the range of 100 – 220 Å. In this case, the FFT satellite peaks are most pronounced and narrow in width, and even a weaker ring of second order satellite peaks becomes visible in the FFT spectra (see inserts of Fig. 1a) – c)). On the other hand, for spacer thicknesses larger than 220 Å, the FFT satellites become increasingly smeared out, and they almost disappear for the superlattice with 330 Å spacers. This indicates an increasing disorder in the dot arrangement. In addition, the corresponding AFM image in Fig. 1f) shows that a second type of smaller PbSe dots appears on the surface in between the widely spaced larger dots. These small dots tend to nucleate in a triangularly ordered manner; and because the 330 Å spacer thickness is already close to the transition to the *fcc*-like dot stacking at 380 Å [4], these interstitial dots obviously represent precursor regions for the *fcc*-like dot stacking in which the lateral dot distances are much smaller than those for the vertically aligned superlattices.

For a more quantitative analysis of the lateral ordering process we have determined the preferred lateral dot spacing L from the separation of the FFT satellite peaks. For the hexagonally ordered samples L can be also calculated from the dot density n using $L = (n \sin 60°)^{-1/2}$. The results are plotted in Fig. 2 as a function of spacer thickness. Clearly, the preferred lateral dot spacing increases strongly with increasing spacer thickness, but it obviously does not follow a strict linear dependence as observed in the case the *fcc*-stacked dot superlattices [2]. With respect to the width of the FFT satellite peaks, there is a clear minimum at a spacer thickness of 160 Å, where the most pronounced lateral dot ordering occurs (Fig. 1 b)). For thinner, as well as thicker, $Pb_{1-x}Eu_xTe$ layers, the FWHM gradually increases from ±16% at d_s = 160Å to about ±21% for d_s = 80Å and 300 Å. Thus, the best hexagonal dot ordering occurs for spacer thicknesses around 160 Å.

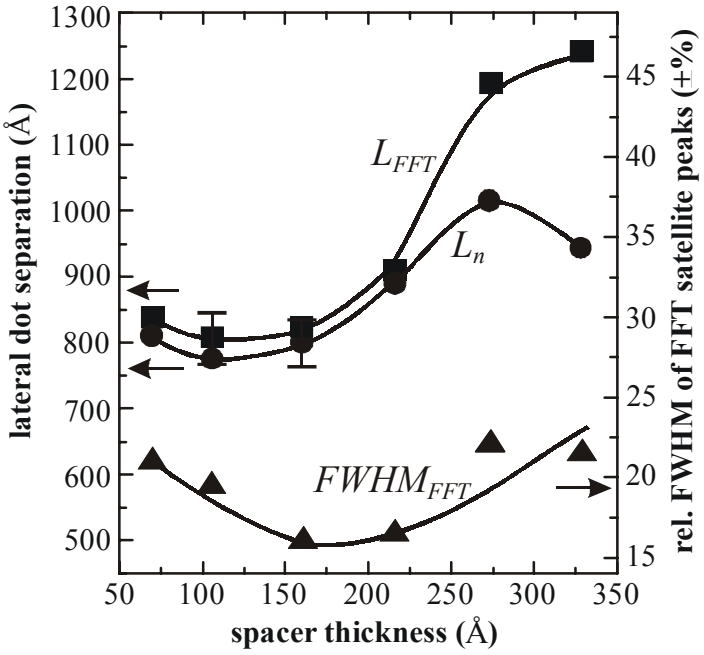

Fig. 2: Lateral dot spacing obtained from the FFT satellite spacings (squares) and the PbSe dot density (circles) plotted as a function of $Pb_{1-x}Eu_xTe$ spacer thickness d_s. Also plotted is the variation of the FWHM (triangles) of the FFT satellite peaks with d_s.

For the well-ordered samples, the average dot separations obtained from the dot densities agree very well with those deduced from the FFT spectra. For spacer thicknesses exceeding 250 Å, however, L_{FFT} becomes significantly larger than the L_n value. This is due to the appearance of the smaller dots in the AFM images. This increases the dot density but does not affect much the preferred separation of the larger dots.

To characterize the dependence of the dot sizes and shapes as a function of SL spacer thickness, we have determined the dot size distributions for all samples. Figure 3 shows representative dot height histograms of the superlattice samples with spacer thicknesses of 160 and 275 Å, as well as that of the single PbSe dot reference layer. The height distribution at d = 160 Å is remarkably narrow (±8%). At a spacer thickness of 275 Å the histogram is strongly shifted to larger height values and a small left hand shoulder (A) starts to emerge at smaller dot heights. This effect is due to the appearance of the additional smaller dots in the AFM images in between the larger dots.

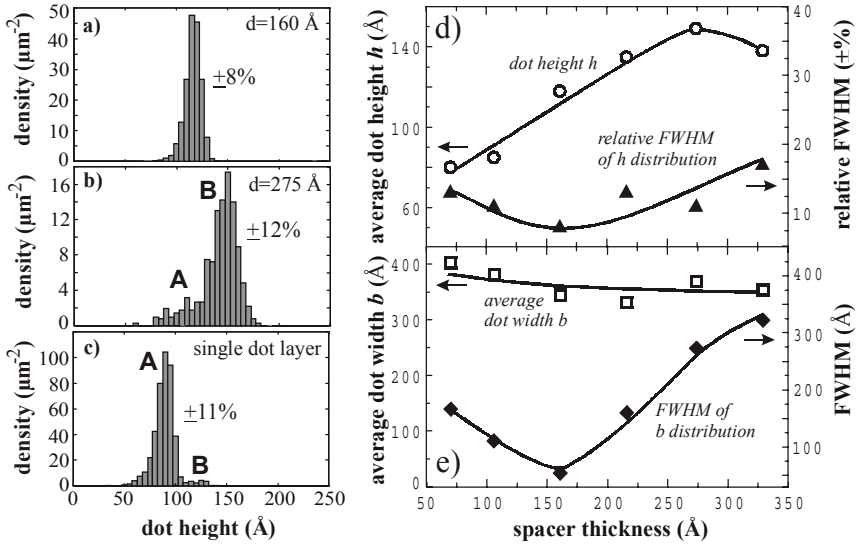

Fig. 3: Left hand side: normalized dot height histograms obtained from the AFM images of Fig. 1 for superlattices with a) 160 and b) 275 Å spacers. The histogram for the 5 ML PbSe single layer reference sample is shown in c). Note the different ordinate scales in the histograms. Right hand side: Average PbSe dot height (d) and width (e) and corresponding FWHM of the size distributions plotted as a function of $Pb_{1-x}Eu_xTe$ spacer thickness.

Figures 3 (d) and (e) summarize the dependence of the average dot height $\bar{h}$ and the dot width b as a function of spacer thickness. The average dot height $\bar{h}$ obtained from the histograms is plotted as a function of spacer thickness. Clearly, up to a spacer thicknesses of 275 Å the height increases essentially linearly with increasing spacer thickness starting from a value of $\bar{h}$ = 80 Å for d = 80 Å to $\bar{h}$ = 149 Å for d = 275 Å, respectively. On the contrary, the dot base width is essentially constant in this range at around 320 Å. Thus, the changes in the dot density induced by the changes in spacer thickness mainly translate into a different vertical dot growth while not affecting much the lateral dot size. From zoomed-in AFM images recorded with selected ultra-sharp AFM tips, it turns out that the dot shapes in the superlattices basically correspond to truncated pyramids with triangular base and {100} side facets. For the very thin spacer layers, the

PbSe dots are rather flat with an aspect ratio of only about 1:5, whereas for the thicker spacers the aspect ratio increases to values around 1:3. This is still significantly smaller than the 1:2.2 aspect ratio of the pyramidal dots of the single PbSe dot layers [2], which do not show any flattening of the island tips. Therefore, the modification in the dot shape in the superlattices must be induced by the elastic strain fields of the buried dots. These are strongest for the thinnest spacers and rapidly decay as its thickness increases.

Perhaps the most interesting feature of our samples is the pronounced narrowing of the size distribution for the ordered superlattice samples. This follows from the dependence of the width of the size distributions also plotted in Figs. 3 (d) and (e) as a function of spacer thickness (full symbols). With respect to the height distributions (Fig. 3 (d)), the statistical variation decreases from ±13% to ±8% for d_s increasing from 80 to 160 Å, after which it increases again to above ±15% for the d_s = 330 Å superlattice. A similar but even more pronounced trend is observed for the statistical variation of the lateral dot widths (Fig. 3 (e)), which again shows a pronounced minimum at a spacer thickness of 160 Å with a rapid increase for thinner as well as thicker spacers. Clearly, this narrowing is most pronounced for the sample with the sharpest FFT satellite peaks, *i.e.*, with the best developed hexagonal order in the dot arrangement. Thus, the size homogenization is a direct consequence of the lateral ordering caused by the elastic interactions during superlattice growth. In addition, it is emphasized that the uniformity of the dots in the d_s = 160 Å superlattice is not only much better than that of the PbSe single dot reference layer (FWHM of the height distribution of ±11%), but it is also as high as the uniformity obtained for trigonally ordered *fcc*-stacked dot superlattices.

4. Conclusions

To conclude, we have demonstrated an efficient lateral ordering of self-assembled vertically aligned PbSe quantum dots superlattices leading to a pronounced narrowing of the size distribution. Furthermore, the adjustment of the superlattice spacer thicknesses provides an effective means for tuning of the lateral dot spacings, the overall dot densities as well as the dot heights, where the latter even show a linear dependence on spacer thickness. This shows that multi-layering is an efficient method for controlling the dimensions and arrangements of self-assembled quantum dots.

This work was supported by the Fonds zur Förderung der wissenschaftlichen Forschung, the Academy of Sciences (APART) and the GME of Austria.

References

[1] J. Tersoff, C. Teichert, and M.G. Lagally, Phys. Rev. Lett. 76, 1675 (1996).

[2] G. Springholz, Holy, M. Pinczolits, and G. Bauer, "Self-Organized Growth of 3D Quantum Dot Superlattice with fcc-like Vertical Stacking and Tunable Lattice Constant", Science 282, 734 (1998).

[3] V. Holy, G. Springholz, M. Pinczolits, G. Bauer, "Strain Induced Vertical and Lateral Correlations in Quantum Dot Superlattices", Phys. Rev. Lett. 83, 356 (1999).

[4] G. Springholz, M. Pinczolits, P. Mayer, V. Holy, G. Bauer, H. Kang, and L. Salmanca-Riba, "Tuning of lateral and vertical correlations in self-organized PbSe/PbEuTe quantum dot superlattices", Phys. Rev. Lett. 84, 4669 (2000).

[5] M. Pinczolits, G. Springholz, and G. Bauer, “Evolution of hexagonal lateral ordering in strain-symmetrized PbSe/PbEuTe quantum dot superlattices”, Phys. Rev. B 60, 11524 (1999).

[6] G. Springholz, T. Schwarzl, W. Heiss, G. Bauer, M. Aigle, and H. Pascher, “Mid infrared surface emitting PbSe/PbEuTe quantum dot lasers”, Appl. Phys. Lett. 79, 1225 (2001).

[7] A. Raab, R. Lechner, G. Springholz “Self-organized lateral ordering for vertically aligned PbSe/PbEuTe quantum dot superlattices”Appl.Phys.Lett. **80**, 1273 (2002).